Construction of bimetallic phosphides nanostructures with in-situ growth, reduction, and phosphidation of ultra-thin graphene layers as highly efficient catalysts towards electrocatalytic oxygen evolution

Dengxia Zhu, Huiting Bi*, Chaolong Wang, Zheng Zhang, Junjiang Zhu*

Hubei Key Laboratory of Biomass Fibers and Eco-dyeing & Finishing, College of Chemistry and Chemical Engineering, Wuhan Textile University, Wuhan, 430200, PR China

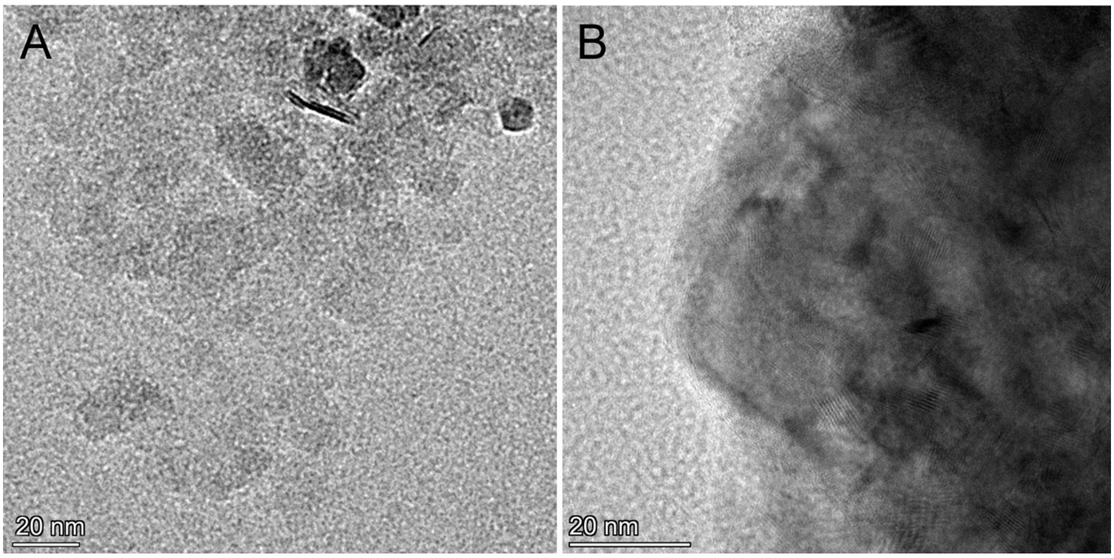

Fig. S1. TEM images of rGO@FeNiSiO$_x$ and rGO@FeNi.

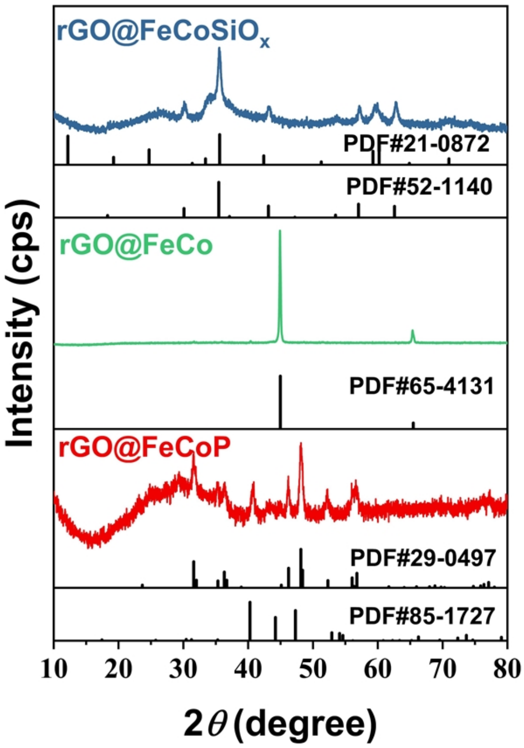

Fig. S2. XRD patterns of rGO@FeCoSiO$_x$, rGO@FeCo, rGO@FeCoP.

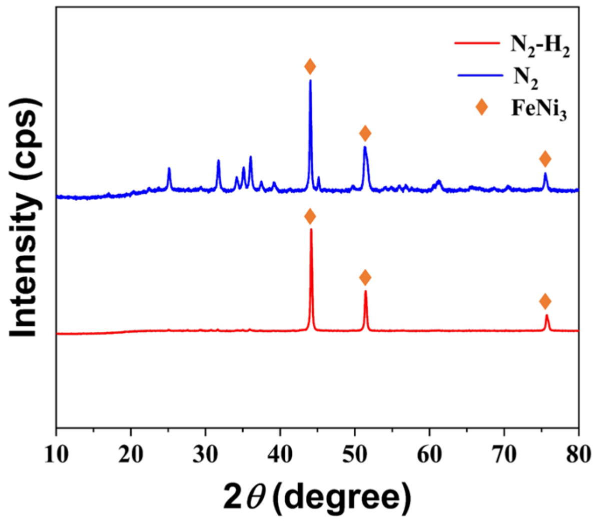

Fig. S3. XRD of catalysts calcined under N_2-H_2 and N_2 atmosphere.

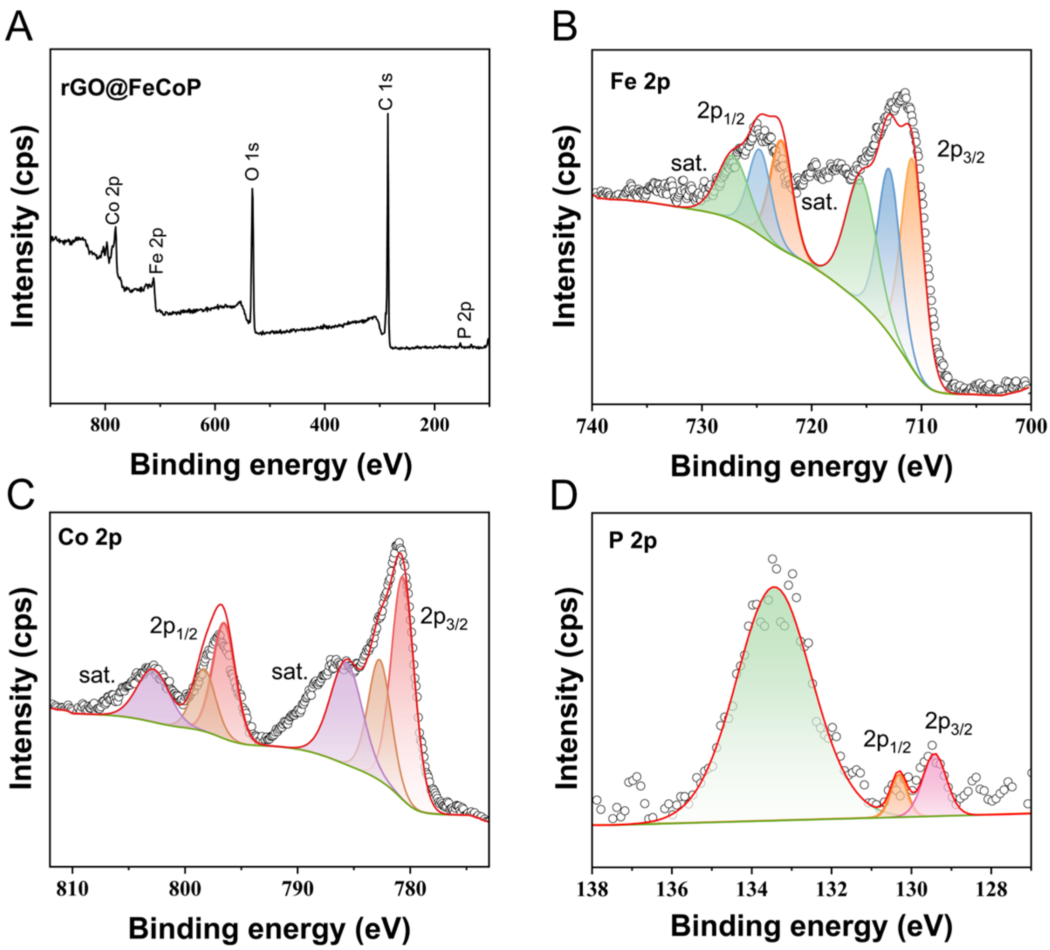

Fig. S4. XPS spectra of rGO@FeCoP (A) survey spectra. (B) Fe 2p. (C) Co 2p. (D) P 2p spectra.

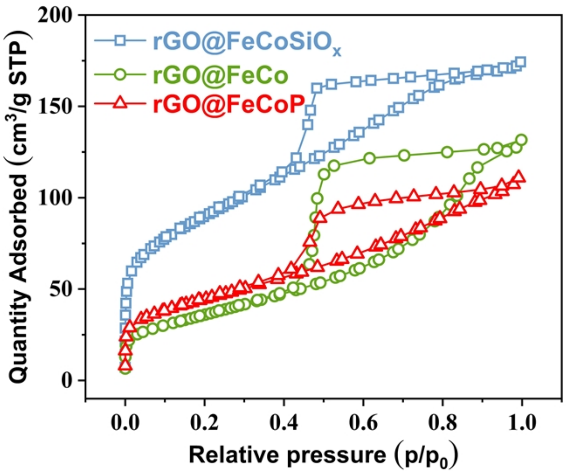

Fig. S5. N_2 adsorption–desorption isotherms of rGO@FeCoSiO$_x$, rGO@FeCo, rGO@FeCoP.

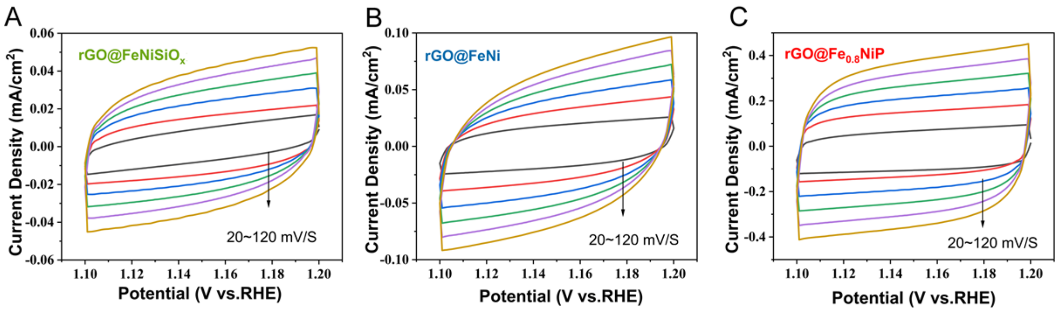

Fig. S6. (A-C) CV curves at different scan rates: 20, 40, 60, 80, 100, and 120 mV s^{-1} from inside to outside.

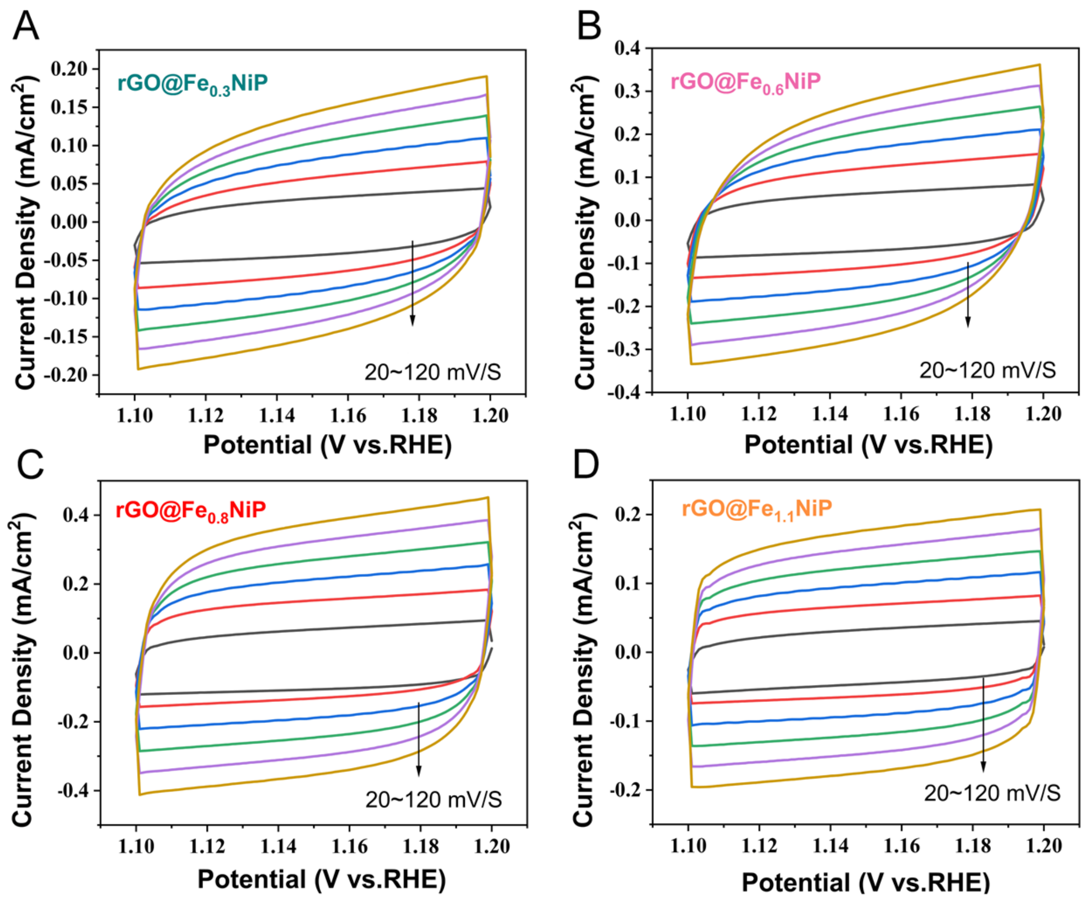

Fig. S7. (A-D) CV curves at different scan rates: 20, 40, 60, 80, 100, and 120 mV s^{-1} from inside to outside.

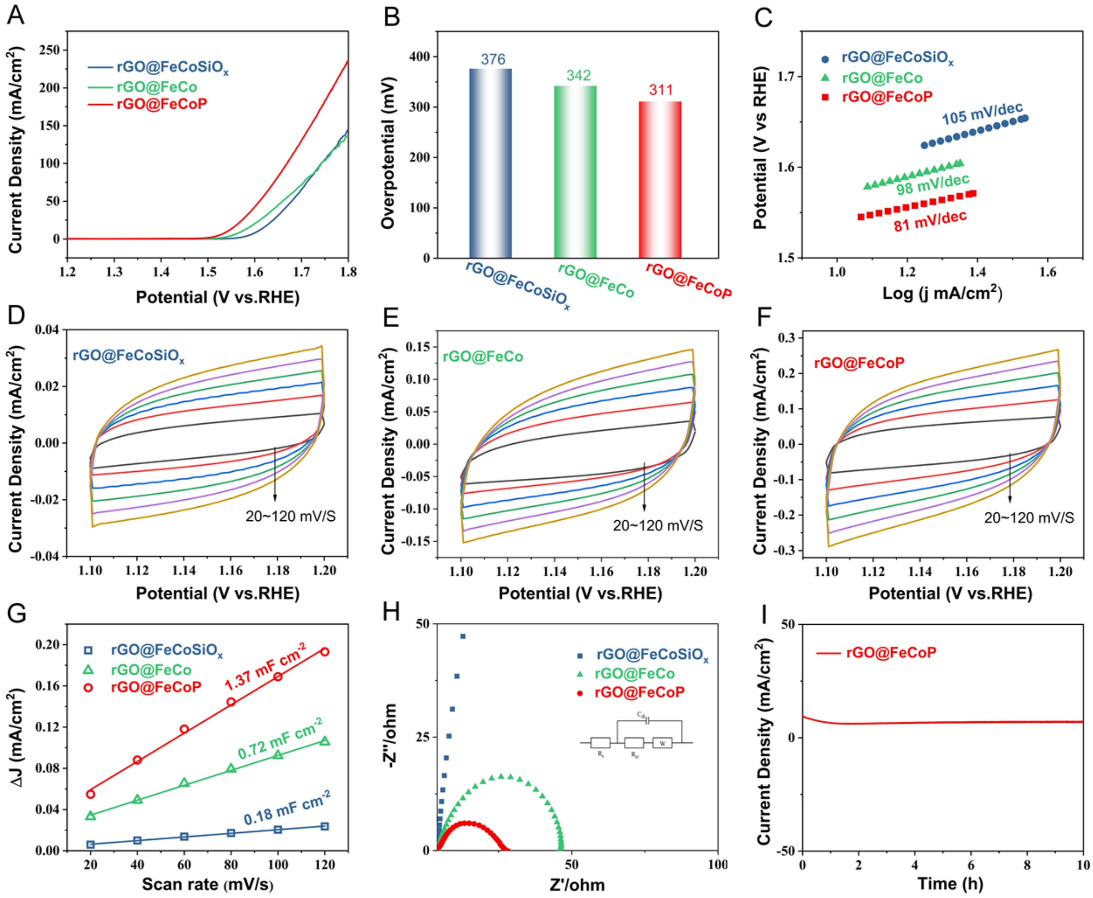

Fig. S8. OER electrocatalytic performance of rGO@FeCoSiO$_x$, rGO@FeCo, rGO@FeCoP. (A) Polarization curves in 1.0 M KOH at a scan rate of 5 mV s^{-1}. (B) Comparison of the overpotentials at the current density of 10 mA cm^{-2}. (C) Corresponding Tafel plots. (D-F) CV curves at different scan rates: 20, 40, 60, 80, 100, and 120 mV s^{-1} from inside to outside. (G) CV current density versus scan Rate. (H) Nyquist plots. (I) Chronopotentiometry curves of rGO@FeCoP at 1.54 V vs. RHE.

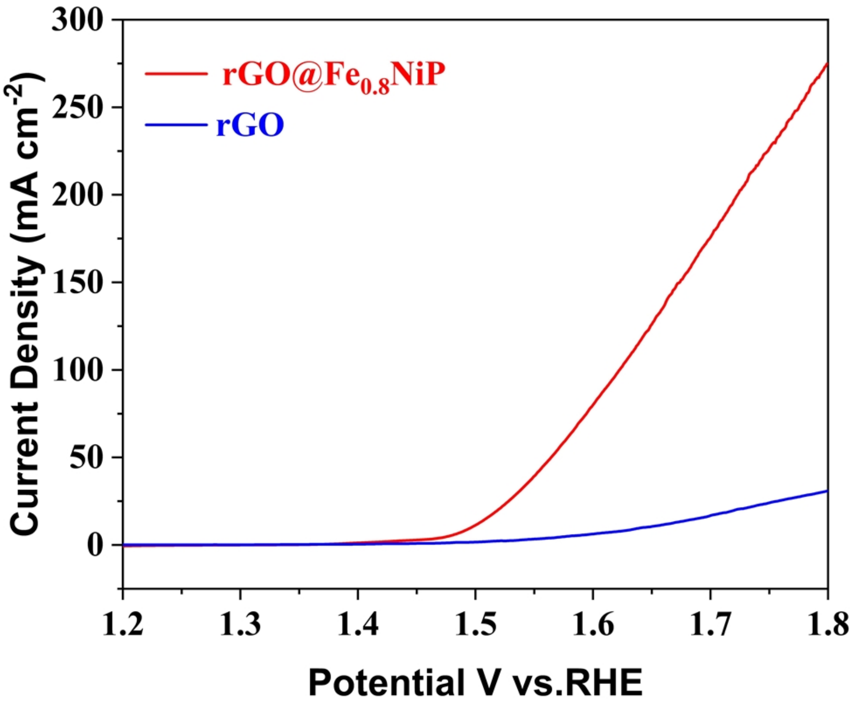

Fig. S9. Polarization curves of rGO@$Fe_{0.8}$NiP and rGO in 1.0 M KOH at a scan rate of 5 mV s^{-1}.

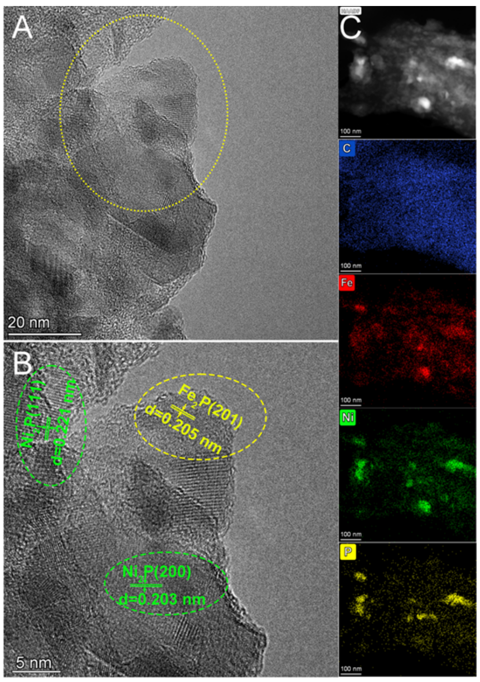

Fig. S10. TEM images (A) and HRTEM images (B) of rGO@FeNiP(recycled), (C) STEM image and EDS elemental mapping of rGO@FeNiP(recycled).

Table S1. OER activity comparison for the samples tested in this work with recently reported catalysts in 1 M KOH.

materials	Electrolyte (M, KOH)	overpotential (mV) at 10 mA/cm^2	refs
rGO@$Fe_{0.8}$Ni-P	1	266	this work
rGO@FeCo-P	1	311	this work
rGO/Co-P	1	333	1
CoPNR/C	1	320	2
Ni_2P@C	1	495	3
FeNiP / NC	1	310	4
NiFeP@NPC	1	350	5
$(Co_{0.54}Fe_{0.46})P_2$	1	370	6
C–$(Co_{0.54}Fe_{0.46})_2P$	0.1	371	7

Table S2. R_{ct} estimated by fitting the equivalent circuit against the EIS data.

materials	$R_{ct}(\Omega)$
rGO@$FeNiSiO_x$	249.1
rGO@FeNi	50.7
rGO@$Fe_{0.8}$NiP	8.6
rGO@$Fe_{0.3}$NiP	18.1
rGO@$Fe_{0.6}$NiP	15.5
rGO@$Fe_{1.1}$NiP	15.8

References

1 P. Li, H. C. Zeng, *ACS Appl. Mater. Interfaces.*, 2019, **11**, 46825-46838.

2 J. Chang, Y. Xiao, M. Xiao, J. Ge, C. Liu and W. Xing, *ACS Catal.*, 2015, **5**, 6874-6878.

3 Q. Kang, M. Li, J. Shi, Q. Lu and F. Gao, *ACS Appl. Mater. Interfaces.*, 2020, **12**, 19447-19456.

4 Y. Du, Y. Han, X. Huai, Y. Liu, C. Wu, Y. Yang and L. Wang, *Int. J. Hydrogen Energy*, 2018, **43**, 22226-22234.

5 F. C. Jian Wang, *Appl. Catal., B*, 2019, **254**, 292-299.

6 A. Mendoza-Garcia, H. Zhu, Y. Yu, Q. Li, L. Zhou, D. Su, M. J. Kramer and S. Sun, *Angewandte Chemie International Edition*, 2015, **54**, 9642-9645.

7 A. Mendoza-Garcia, D. Su and S. Sun, *Nanoscale*, 2016, **8**, 3244-3247.